



Note

Ionic iridium complex coordinated with tetrathiafulvalene-fused phenanthroline ligand: Synthesis, photophysical, electrochemical and electrochemiluminescence properties



Jie Qin^{a,c,*}, Sheng-Yuan Deng^{b,d,1}, Chen-Xi Qian^c, Tian-Yi Li^c, Huang-Xian Ju^d, Jing-Lin Zuo^c

^a School of Life Science, Shandong University of Technology, Zibo 255049, PR China

^b School of Environmental and Biological Engineering, Nanjing University of Science and Technology, Nanjing 210094, PR China

^c State Key Laboratory of Coordination Chemistry, School of Chemistry and Chemical Engineering, Nanjing University, Nanjing 210093, PR China

^d State Key Laboratory of Analytical Chemistry for Life Science, School of Chemistry and Chemical Engineering, Nanjing University, Nanjing 210093, PR China

ARTICLE INFO

Article history:

Received 5 August 2013

Received in revised form

22 October 2013

Accepted 23 October 2013

Keywords:

Cationic iridium complex

Tetrathiafulvalene ligand

Photoluminescence

Electrochemiluminescence

ABSTRACT

A new cationic iridium(III) complex salt, $[\text{Ir}(\text{ppy})_2(\text{L})]\text{PF}_6$ ($\text{ppy} = 2\text{-phenylpyridine}$) (**1**), was synthesized by using tetrathiafulvalene fused 4',5'-dimethyldithiotetrathiafulvenyl[4,5-f][1,10]phenanthroline (**L**) as NN ancillary ligand. The photophysical, electrochemical and electrochemiluminescence (ECL) behavior of the complex are investigated. Complex **1** is found to be emissive at room temperature with the λ_{max} value at 607 nm. It is expected that this new luminescent complex **1** would be further explored for promising applications in functional emitting material.

© 2013 Elsevier B.V. All rights reserved.

1. Introduction

During the past decades, a lot of attention has been devoted to the design and synthesis of tetrathiafulvalene (TTF) derivatives since their excellent potential application in molecule-scale electronics and devices [1–5]. Among them, one of growing research interest is the combination of the electrochemically active properties of organic TTF units with magnetic or optical properties of inorganic metal ions to obtain new multifunctional molecular materials. Under this strategy, a variety of functional groups which are tailored for coordination toward diverse transition metal ions have been grafted to the TTF core [6–9]. Recently, we have reported the facile synthesis and properties of the chelating ligand, 4',5'-dimethyldithiotetrathiafulvenyl[4,5-f][1,10]phenanthroline (**L**) [10], which is first described by Shatruk's group [7b].

Due to their relatively short lifetime, significant Stokes shifts, and remarkable structure–function relationships, phosphorescent iridium(III) complexes have widely been employed in organic

light-emitting diodes (OLEDs) devices [11], chemical sensors [12], fluorescent imaging [13], etc. Meanwhile as an important class of inorganic luminescent systems, iridium(III) complexes have also attracted wide interest in electrochemiluminescence (ECL) that the luminescence is generated by an electrochemical reaction without additional excitation source [14,15].

As an extension of our work, we investigated the reaction of the versatile TTF ligand **L** with cyclometalated iridium(III) complex. The unique π electron delocalized nature of TTF unit undergoing mix-valence state would allow the efficient incorporation of iridium luminophore into functional organic semiconductor. To date, only one paper on iridium(III) complex with tetrathiafulvalene fused ligand is reported [16]. Herein, we report the synthesis, characterization, electrochemical, photophysical and ECL behaviors of cationic iridium(III) complex, $[\text{Ir}(\text{ppy})_2(\text{L})]\text{PF}_6$ (**1**), which is based on tetrathiafulvalene fused phenanthroline (**L**) as NN ancillary ligand.

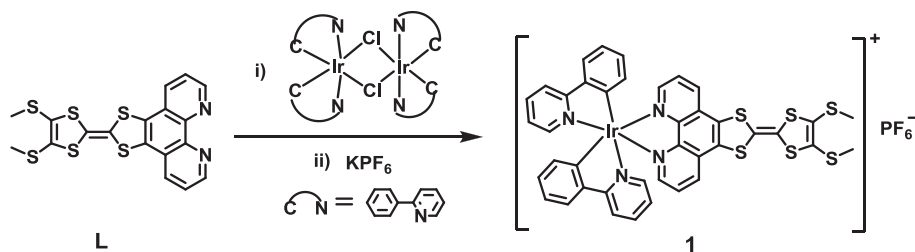
2. Results and discussion

Cationic iridium(III) complex **1** was prepared in good yield via a two-step procedure (Scheme 1) similar to the synthesis of $[\text{Ir}(\text{ppy})_2(\text{phen})]\text{PF}_6$ ($\text{phen} = \text{phenanthroline}$) (**2**) [11b,17]. It was characterized by elemental analysis, IR, ^1H NMR and electro spray

* Corresponding author. School of Life Science, Shandong University of Technology, Zibo 255049, PR China. Tel.: +86 533 2780271.

E-mail address: qinjetutu@163.com (J. Qin).

¹ These authors contributed equally to this work.

Scheme 1. Synthetic routes to complex **1**.

ionization mass spectrometry (Figs. S1 and S2). Compared with the synthesis of neutral iridium(III) complex based on TTF-fused diketone ligand [16], which needs harsh reaction conditions and much longer reaction time, the synthesis of **1** is carried out under mild reaction conditions with higher yield.

The electrochemical properties of **L** and **1** investigated by cyclic voltammetry is present in Fig. 1. The first two reversible oxidations of **1** at $E_{1/2}^1 = 0.90$ and $E_{1/2}^2 = 1.13$ V (vs. Ag/AgCl) are ascribed to the successive reversible oxidation of neutral TTF backbone to the radical cation and then to the dication form. As a result of the electron-withdrawing inductive effect of the Ir^{III} core, these two oxidation potentials are positively shifted compared with **L** ($E_{1/2}^1 = 0.81$ V, $E_{1/2}^2 = 1.09$ V, vs. Ag/AgCl). While the oxidation wave of Ir^{III} core is not observed which is probably attributed to the electrostatic interactions between the TTF²⁺ moiety and the Ir^{III} core [16].

As depicted in Fig. 2, the absorption spectrum of complex **1** shows the following features: intense absorption bands below 350 nm, which are characteristic of the spin-allowed intraligand ($\pi \rightarrow \pi^*$) (LC) transition; moderately intense absorption bands in the range 350–450 nm and weak absorption bands above 450 nm are also observed, which can be generally assigned to charge transfer (CT) transition. To rationalize the electronic absorption spectrum of **1**, a detailed computational study has been performed [18,19].

Analyses of TD-DFT calculations reveal qualitative agreement with experimental absorption data (Fig. 2). The most representative molecular frontier orbital diagrams are shown in Fig. 3. Table 1 summarizes the spin-allowed electronic transitions. The TD-DFT calculations for **1** in gas phase suggest a weak electronic transition from TTF-based HOMO to mainly phen-based LUMO + 1 with an absorption band at 482 nm, which is approximate to the

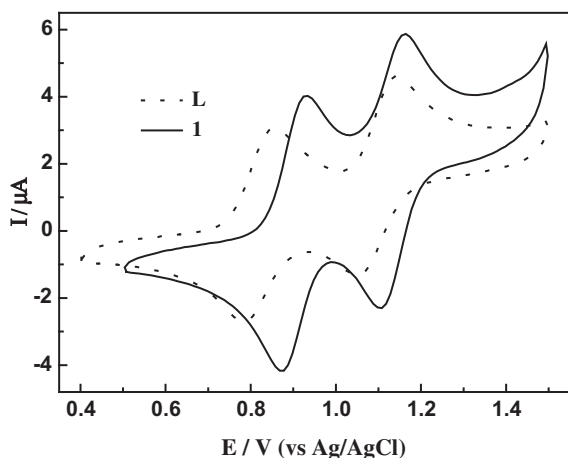


Fig. 1. Cyclic voltammograms of compounds **1** and **L** (5×10^{-4} M) in $\text{CH}_2\text{Cl}_2/\text{CH}_3\text{CN}$ solution (1:1, v/v) of $n\text{-Bu}_4\text{NClO}_4$ (0.1 M) at a sweep rate of 100 mV/s.

experimental spectral data of 475 nm. Thus the lowest-energy absorption band in **1** can be assigned to intraligand charge transfer (ILCT) from the electron-donor TTF core to the electron-acceptor phen unit, whereas the moderate absorption bands centered at 370 nm are found as the electronic transitions from orbitals (HOMO – 2 and HOMO – 4) to phen-localized LUMO. These electronic transitions have Metal–Ligand Charge Transfer (MLCT, $d\pi_{\text{Ir}} \rightarrow \pi^*_{\text{phen}}$) and Ligand–Ligand Charge Transfer (LLCT, $\pi_{\text{ppy}} \rightarrow \pi^*_{\text{phen}}$) character. The strong absorption peak in the ultraviolet region is mainly correlated to the electronic transitions from HOMO – 10 to LUMO + 1 and HOMO – 2 to LUMO + 5 and characteristic of $\pi_{\text{phen}}/\pi_{\text{TTF}} \rightarrow \pi^*_{\text{phen}}/\pi^*_{\text{TTF}}$ ILCT and $\pi_{\text{ppy}} \rightarrow \pi^*_{\text{ppy}}/\pi^*_{\text{phen}}/\pi^*_{\text{TTF}}$ ILCT.

The UV–vis–NIR spectra of complex **1** upon addition of oxidant nitrosonium hexafluorophosphate (NOPF₆) in CH_2Cl_2 solution was also investigated. As shown in Fig. 4, upon the addition of 1.0 equiv of oxidant NOPF₆, a new weak broad band centered at 832 nm is observed, which results from the characteristic absorption band of the cationic radical TTF^{•+} [10,16], meanwhile, the initial absorbance at $\lambda = 262$ nm and 298 nm decrease. After the further oxidation with 1.0 equiv of NOPF₆, the TTF unit is oxidized to the dicationic state, the characteristic absorption band of TTF^{•+} disappears, and the absorption bands in the range 420–600 nm decrease. These phenomena are similar with the oxidation of the neutral TTF–Ir complex [16].

Unlike the rhenium complex $\text{ClRe}(\text{CO})_3(\text{L})$ we reported before [10], complex **1** is luminescent at room temperature in dichloromethane solution which can be ascribe to the different photo-induced electron transfer efficiencies of the TTF unit. The corresponding photoluminescence data of complex **1** are summarized in Table 2. Fig. 5 shows the photoluminescence spectra in different conditions. Figs. S3–S5 show the lifetime curves of **1** in different solvent.

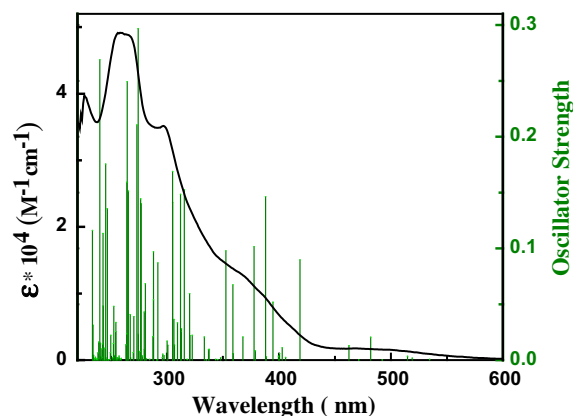


Fig. 2. Electronic absorption spectrum of **1** in CH_2Cl_2 solution together with the calculated oscillator strengths.

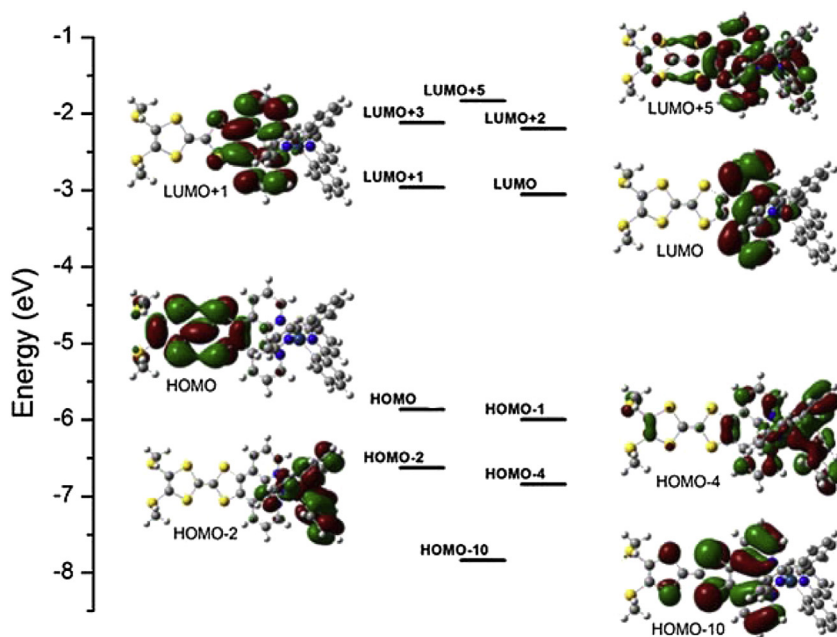
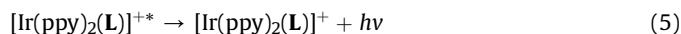
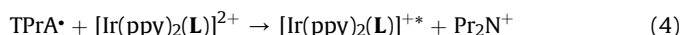
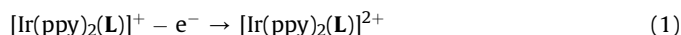


Fig. 3. Selected molecular orbitals energy diagram and graphical representation for frontier molecular orbitals of **1**.

Upon excitation at 380 nm, complex **1** exhibits broad structureless band at about 607 nm in CH₂Cl₂ solution. According to the previous study, emission bands from LC states usually display vibronic progressions, while those from MLCT states are broad and featureless. Meanwhile, the MLCT states are known to be strongly temperature and solvent dependent [17,20]. For complex **1**, a blue shift in the emission maxima about 41 nm with additional structure on going from fluid solution at room temperature to a rigid matrix at 77 K was observed (Fig. 5). And the emission maximum value occurs at higher energy in CH₂Cl₂ than that in more polar THF or CH₃CN indicating that the excited state possesses a dominant MLCT character (Fig. 5). Thus we conclude that the emission of **1** gains larger contributions from MLCT state. With the 1.0 equiv of oxidant NOPF₆ added, the emission intensity is remarkably decreased, and reaches the minimum after the addition of another 1.0 equiv of NOPF₆ (Fig. S6), which is probably caused by photo-induced electron transfer from Ir^{III} core to the oxidized TTF moiety.

The ECL performance of free ligand **L**, complex **1** and reference complex [Ir(ppy)₂(phen)]PF₆ (**2**) were studied in CH₂Cl₂ solution containing *n*-Bu₄NClO₄ as the supporting electrolyte and tri-*n*-propylamine (TPrA) as the coreactant. The typical ECL profile registered during a cyclic voltammetry is shown in Fig. 6. All the three compounds show broad oxidation peak, indicating the overlapped oxidation process. The ligand **L** is non-luminous, while for complex **1** and **2**, the ECL emission occurs due to the reaction of Ir^{III} core with TPrA radical, following the classic oxidative-reduction coreactant mechanism (Eqs. (1)–(5)) [14,15]. The ECL peak

intensity of complex **1** is half that of complex **2**, whose ECL emission occurs at higher potential. To examine the peak wavelength of ECL emission, the corresponding ECL spectrum of complex **1** is also achieved. As shown in Fig. 7, the maximum emission is about 627 nm, indicating the formation of the same excited state in photoluminescence and ECL.



3. Conclusion

In conclusion, the air-stable cationic-functionalized iridium(III) complex **1** based on tetrathiafulvalene-fused phenanthroline as NN ancillary ligand is successfully synthesized and characterized. The electronic transition spectrum of **1** is calculated with TD-DFT, and a good agreement with the experimental data is observed. Interestingly, **1** is phosphorescent with maximum emission wavelength at 607 nm, and the ECL result shows the same excited state as photoluminescence. Complex **1**

Table 1
Main experimental and calculated optical transitions for **1**.

Orbital excitations	Transition	Character	Oscillation strength	Calcd (nm)	Exptl (nm)
HOMO → LUMO + 1	ILCT	$\pi_{\text{TTF}} \rightarrow \pi_{\text{phen}}^*$	0.0198	482	475
HOMO - 2 → LUMO	MLCT/LLCT	$d\pi_{\text{Ir}}/\pi_{\text{ppy}} \rightarrow \pi_{\text{phen}}^*$	0.0632	418	
HOMO - 4 → LUMO	MLCT/LLCT	$d\pi_{\text{Ir}}/\pi_{\text{ppy}} \rightarrow \pi_{\text{phen}}^*$	0.1577	387	370
HOMO - 10 → LUMO + 1	ILCT	$\pi_{\text{phen}}/\pi_{\text{TTF}} \rightarrow \pi_{\text{phen}}^*/\pi_{\text{TTF}}^*$	0.1617	304	298
HOMO - 2 → LUMO + 5	ILCT	$\pi_{\text{ppy}} \rightarrow \pi_{\text{ppy}}^*/\pi_{\text{phen}}^*/\pi_{\text{TTF}}^*$	0.2905	274	262

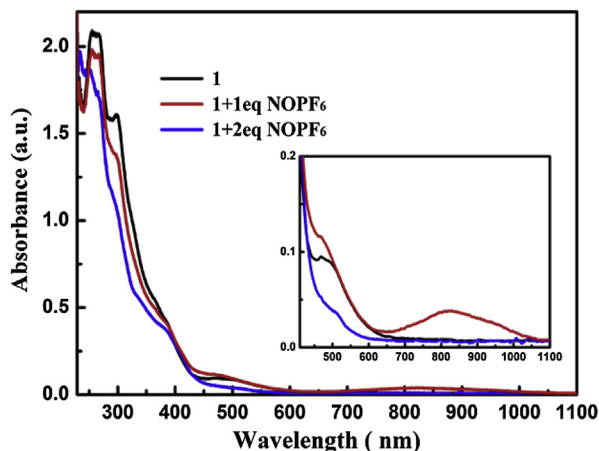


Fig. 4. Absorption spectra for **1** in CH_2Cl_2 upon the addition of NOPF_6 . The near-infrared absorption transitions are magnified in the inset.

may be useful as photoelectric functional material, and more work is going on in our laboratory.

4. Experimental section

4.1. General procedures

The IR spectra were taken on a Vector22 Bruker spectrophotometer ($400\text{--}4000\text{ cm}^{-1}$) with KBr pellets. ^1H NMR spectra were measured on a Bruker AM 500 spectrometer. Chemical shifts were reported in ppm relative to Me_4Si as internal standard. Elemental analyses for C, H and N were performed on a Perkin–Elmer 240C analyzer. Electrospray ionization mass spectrometry (ESI-MS) spectra were determined with LCQ Fleet instrument with CH_3CN as a solvent. Cyclic voltammograms (CV) were recorded on an Im6eX electrochemical analytical instrument, with a polished Pt plate as the working electrode, a Pt foil as the counter electrode, Ag/AgCl as the reference electrode, and $0.1\text{ M } n\text{-Bu}_4\text{NClO}_4$ as the supporting electrolyte. All the potentials were run at scan rates of 100 mV/s . UV–vis spectra were measured on a Shimadzu UV-3100 spectrophotometer. Photoluminescence spectra and photoluminescence lifetime measurement were carried out on an LS 55 and an Edinburgh Instruments FLS920P fluorescence spectrometer spectrometer, respectively. The solution was degassed by three freeze–pump–thaw cycles. ECL behavior was studied on MPI-E multifunctional electrochemical and chemiluminescent system (Xi'an Remex Analytical Instrument Ltd. Co., China) at room temperature with bare glassy carbon electrode as the working electrode. For ECL experiment in $1\text{ mM } \text{CH}_2\text{Cl}_2$ of **1**, tri-*n*-propylamine (10 mM) was added as the coreactant, and $0.1\text{ M } n\text{-Bu}_4\text{NClO}_4$ was used as the supporting electrolyte. The ECL spectrum was collected with an Edinburgh FLS920 fluorescence spectrometer (Livingston, UK) by electrolyzing CH_2Cl_2 solution containing 1 mM of **1**, $0.1\text{ M } n\text{-Bu}_4\text{NCl}$ and 10 mM TPrA in a self-designed quartz cuvette at $+2.0\text{ V}$ upon a polished bare glassy carbon electrode via amperometric $i\text{--}t$ curve.

Table 2
Photoluminescent data of complex **1**.

Complex	Medium (T/K)	λ_{max} (nm)	Φ_{em}	τ (ns)
1	CH_2Cl_2 (298)	607	0.017	410.9
	THF (298)	620	0.0054	75.9
	CH_3CN (298)	632	0.012	158.5
	glass (77)	566	–	–

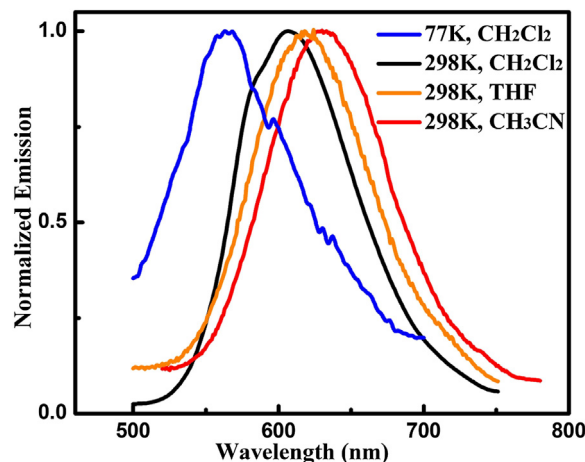


Fig. 5. Photoluminescence spectra of **1** in different conditions ($\lambda_{\text{ex}} = 380\text{ nm}$) under argon atmosphere.

The luminescence quantum efficiencies were calculated by comparison of the fluorescence intensities (integrated areas) of a standard sample $\text{Ir}(\text{ppy})_3$ and complex **1** according to Eq. (6) [22].

$$\Phi_{\text{unk}} = \Phi_{\text{std}} \left(\frac{I_{\text{unk}}}{I_{\text{std}}} \right) \left(\frac{A_{\text{std}}}{A_{\text{unk}}} \right) \left(\frac{\eta_{\text{unk}}}{\eta_{\text{std}}} \right)^2 \quad (6)$$

where Φ_{unk} is the luminescence quantum yield of the complex **1**, Φ_{std} is the luminescence quantum yield of $\text{Ir}(\text{ppy})_3$ solution, I_{unk} and I_{std} are the integrated fluorescence intensities of the complex **1** and $\text{Ir}(\text{ppy})_3$, respectively. A_{unk} and A_{std} are the absorbances of the complex **1** and $\text{Ir}(\text{ppy})_3$ at excitation wavelengths. The η_{unk} and η_{std} terms represent the refractive indices of the corresponding solvents (pure solvents were assumed). The Φ_{std} value of $\text{Ir}(\text{ppy})_3$ has been revalued to be 0.4 [23].

4.2. Materials

All solvents were dried by standard methods and distilled prior to use. Solvents used for electrochemistry and spectroscopy were spectroscopic grade. Moisture-sensitive reactions were carried out under a nitrogen atmosphere. 4',5'-Dimethyldithio-tetrathiafulvenyl[4,5-f][1,10]phenanthroline (**L**), and cyclometalated iridium chlorobridged dimer $[\text{Ir}(\text{ppy})_2\text{Cl}]_2$ ($\text{ppy} = 2\text{-phenylpyridine}$) were synthesized according to the published procedures [10,11b,21].

4.3. Syntheses

4.3.1. $[\text{Ir}(\text{ppy})_2(\text{L})]\text{PF}_6$ (**1**)

Under a nitrogen atmosphere, a mixture of **L** (61 mg, 0.14 mmol) and $[\text{Ir}(\text{ppy})_2\text{Cl}]_2$ (72 mg, 0.067 mmol) in 13 mL of CH_2Cl_2 and 5 mL of CH_3OH was refluxed for 4 h. Then the dark red solution was cooled to room temperature, and 8-fold excess of potassium hexafluorophosphate was added. The suspension was stirred for another 2 h and then was filtered. The filtrate was evaporated to dryness under reduced pressure. Purification was made by flash chromatography on a silica gel column using $\text{CH}_2\text{Cl}_2/\text{MeOH}$ ($v/v = 80:1$) as the eluent to afford dark red crystalline solid in 80% yield. IR (KBr, cm^{-1}): 2920, 1607, 1582, 1478, 1420, 1314, 1267, 1163, 1062, 940, 841, 757, 722, 556. ^1H NMR (500 MHz, CD_2Cl_2): δ 8.30 (d, $J = 5.0\text{ Hz}$, 2H), 8.23 (d, $J = 8.5\text{ Hz}$, 2H), 7.97 (d, $J = 8.5\text{ Hz}$, 2H), 7.83 (dd, $J = 5.5\text{ Hz}$, 8.5 Hz, 2H), 7.77 (d, $J = 8.5\text{ Hz}$, 4H), 7.35 (d, $J = 5.5\text{ Hz}$, 2H), 7.11 (t, $J = 7.5\text{ Hz}$, 2H), 7.00 (t, $J = 7.5\text{ Hz}$, 2H), 6.91 (t, $J = 6.5\text{ Hz}$,

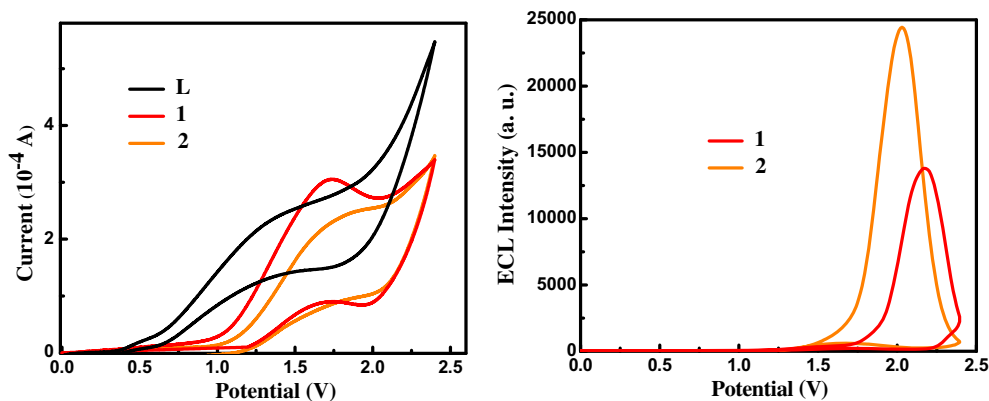


Fig. 6. Cyclic voltammogram and corresponding ECL signal of compound **L**, **1** and **2** in CH_2Cl_2 solution (1 mM) at room temperature containing 0.1 M $n\text{-Bu}_4\text{NClO}_4$ as the supporting electrolyte and 10 mM TPrA as the coreactant at room temperature. PMT bias: -700 V, scan rate: 100 mV/s.

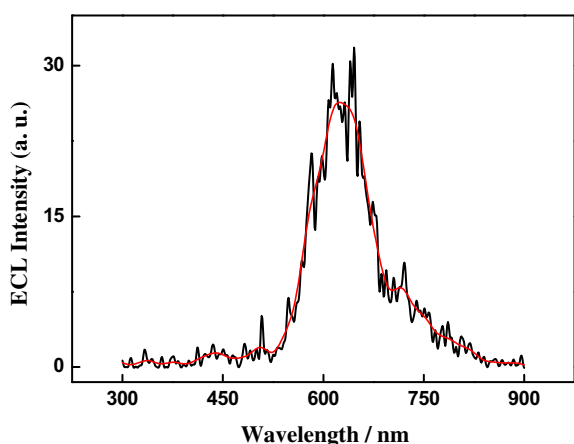


Fig. 7. ECL spectra of compound **1** in CH_2Cl_2 solution (1 mM) containing 0.1 M $n\text{-Bu}_4\text{NClO}_4$ as the supporting electrolyte and 10 mM TPrA as the coreactant at room temperature. The black line is the experimental line and the red is the smoothing line. (For interpretation of the references to color in this figure legend, the reader is referred to the web version of this article.)

2H), 6.39 (d, $J = 7.5$ Hz, 2H), 2.45 (s, 6H). MS (ESI-MS): m/z 949.17 $[\text{M} - \text{PF}_6]^+$, 144.92 PF_6^- . Anal. Calcd for $\text{C}_{40}\text{H}_{28}\text{S}_6\text{N}_4\text{PF}_6\text{Ir}$: C, 43.90; H, 2.58; N, 5.12. Found: C, 44.23; H, 2.24; N, 5.38%.

4.4. Computational details

The calculations were carried out with Gaussian 03 Program Package [18]. DFT and TD-DFT methods with no symmetry constraints were employed with the B3LYP. The LANL2DZ basis set was used to treat the iridium atom, the 6-31G* basis set was used to treat all other atoms.

Acknowledgments

This work was supported by the National Natural Science Foundation of China (21301108 and 51173075).

Appendix A. Supplementary data

Supplementary data related to this article can be found at <http://dx.doi.org/10.1016/j.jorganchem.2013.10.041>.

References

- [1] (a) J. Ferraris, D.O. Cowan, V.V. Walatka, J.H. Perlstein, *J. Am. Chem. Soc.* 95 (1973) 948–949; (b) H. Tanaka, Y. Okano, H. Kobayashi, W. Suzuki, A. Kobayashi, *Science* 291 (2001) 285–287.
- [2] G. Ho, J.R. Heath, M.R. Bryce, *Chem. Eur. J.* 11 (2005) 2914–2922.
- [3] (a) M. Mas-Torrent, M. Durkut, P. Hadley, *J. Am. Chem. Soc.* 126 (2004) 984–985; (b) Z.M. Wei, H.X. Xi, H.L. Dong, L.J. Wang, W. Xu, W.P. Hu, D.B. Zhu, *J. Mater. Chem.* 20 (2010) 1203–1207.
- [4] (a) N. Martín, L. Sánchez, D.M. Guldi, *Chem. Commun.* (2000) 113–114; (b) A. Molina-Ontoria, G. Fernandez, M. Wielopolski, *J. Am. Chem. Soc.* 131 (2009) 12218–12229.
- [5] (a) H.Y. Lu, W. Xu, D.Q. Zhang, C.F. Chen, D.B. Zhu, *Org. Lett.* 7 (2005) 4629–4632; (b) J. Xiong, L. Sun, Y. Liao, G.N. Li, J.L. Zuo, X.Z. You, *Tetrahedron Lett.* 52 (2011) 6157–6161.
- [6] (a) F. Iwahori, S. Gohlen, L. Ouahab, R. Carlier, J.P. Sutter, *Inorg. Chem.* 40 (2001) 6541–6542; (b) F. Setifi, L. Ouahab, S. Golhen, Y. Yoshida, G. Saito, *Inorg. Chem.* 42 (2003) 1791–1793; (c) S.X. Liu, C. Ambrus, S. Dolder, A. Neels, S. Decurtins, *Inorg. Chem.* 45 (2006) 9622–9624.
- [7] (a) K. Hervé, S.X. Liu, O. Cadot, S. Golhen, Y.L. Gal, A. Bousseksou, H. Stoeckli-Evans, S. Decurtins, L. Ouahab, *Eur. J. Inorg. Chem.* (2006) 3498–3502; (b) L.K. Keniley Jr., L. Ray, K. Kovnir, L.A. Dellinger, J.M. Hoyt, M. Shatruk, *Inorg. Chem.* 49 (2010) 1307–1309; (c) Y.F. Ran, S.X. Liu, O. Sereda, A. Neels, S. Decurtins, *Dalton Trans.* 40 (2011) 8193–8198.
- [8] (a) F. Pointillart, Y.L. Gal, S. Golhen, O. Cadot, L. Ouahab, *Chem. Commun.* (2009) 3777–3779; (b) Y.R. Qin, Q.Y. Zhu, L.B. Huo, Z. Shi, G.Q. Bian, J. Dai, *Inorg. Chem.* 49 (2010) 7372–7381; (c) T.L.A. Nguyen, T. Devic, P. Mialane, E. Rivière, A. Sonner, N. Stock, R. Demir-Cakan, M. Morcrette, C. Livage, J. Marrot, J.M. Tarascon, G. Férey, *Inorg. Chem.* 49 (2010) 10710–10717.
- [9] J. Massue, N. Bellec, S. Chopin, E. Levillain, T. Roisnel, R. Clérac, D. Lorcy, *Inorg. Chem.* 44 (2005) 8740–8748.
- [10] J. Qin, L. Hu, G.N. Li, X.S. Wang, Y. Xu, J.L. Zuo, X.Z. You, *Organometallics* 30 (2011) 2173–2179.
- [11] (a) Y.C. Zhu, L. Zhou, H.Y. Li, Q.L. Xu, M.Y. Teng, Y.X. Zheng, J.L. Zuo, H.J. Zhang, X.Z. You, *Adv. Mater.* 23 (2011) 4041–4046; (b) R.D. Costa, E. Ortí, H.J. Bolink, S. Gräber, S. Schaffner, M. Neuburger, C.E. Housecroft, E.C. Constable, *Adv. Funct. Mater.* 19 (2009) 3456–3463; (c) M.S. Lowry, S. Bernhard, *Chem. Eur. J.* 12 (2006) 7970–7977; (d) S. Fantacci, F. De Angelis, *Coord. Chem. Rev.* 255 (2011) 2704–2726.
- [12] (a) W.J. Xu, S.J. Liu, X.Y. Zhao, S. Sun, S. Cheng, T.C. Ma, H.B. Sun, Q. Zhao, W. Huang, *Chem. Eur. J.* 16 (2010) 7125–7133; (b) W.J. Xu, S.J. Liu, H.B. Sun, X.Y. Zhao, Q. Zhao, S. Sun, S. Cheng, T.C. Ma, L.X. Zhou, W. Huang, *J. Mater. Chem.* 21 (2011) 7572–7581; (c) V. Guerschais, J.L. Fillaut, *Coord. Chem. Rev.* 255 (2011) 2448–2457; (d) K.K.W. Lo, K.Y. Zhang, S.P.Y. Li, *Pure Appl. Chem.* 83 (2011) 823–840.
- [13] (a) M.X. Yu, Q. Zhao, L.X. Shi, F.Y. Li, Z.G. Zhou, H. Yang, T. Yi, C.H. Huang, *Chem. Commun.* (2008) 2115–2117; (b) Q. Zhao, M.X. Yu, L.X. Shi, S.J. Liu, C.Y. Li, M. Shi, Z.G. Zhou, C.H. Huang, F.Y. Li, *Organometallics* 29 (2010) 1085–1091; (c) R. Vankayala, G. Gollavelli, B.K. Mandal, *J. Mater. Sci. Mater. Med.* 24 (2013) 1993–2000; (d) K.K.W. Lo, K.Y. Zhang, *Adv. Mater.* 2 (2012) 12069–12083.

- [14] (a) M.M. Richter, *Chem. Rev.* 104 (2004) 3003–3036;
(b) L.Z. Hu, G.B. Xu, *Chem. Soc. Rev.* 39 (2010) 3275–3304.
- [15] (a) S. Zanarini, M. Felici, G. Valenti, M. Marcaccio, L. Prodi, S. Bonacchi, P. Contreras-Carballada, R.M. Williams, M.C. Feiters, R.J.M. Nolte, L.D. Cola, F. Paolucci, *Chem. Eur. J.* 17 (2011) 4640–4647;
(b) C.X. Li, J. Lin, X.Y. Yang, J. Wan, *J. Organomet. Chem.* 696 (2011) 2445–2450.
- [16] C.H. Xu, W. Sun, C. Zhang, C. Zhou, C.J. Fang, C.H. Yan, *Chem. Eur. J.* 15 (2009) 8717–8721.
- [17] Q. Zhao, S.J. Liu, M. Shi, F.Y. Li, H. Jing, T. Yi, C.H. Huang, *Organometallics* 26 (2007) 5922–5930.
- [18] M.J. Frisch, G.W. Trucks, H.B. Schlegel, G.E. Scuseria, M.A. Robb, J.R. Cheeseman, J.A. Montgomery Jr., T. Vreven, K.N. Kudin, J.C. Burant, J.M. Millam, S.S. Iyengar, J. Tomasi, V. Barone, B. Mennucci, M. Cossi, G. Scalmani, N. Rega, G.A. Petersson, H. Nakatsuji, M. Hada, M. Ehara, K. Toyota, R. Fukuda, J. Hasegawa, M. Ishida, T. Nakajima, Y. Honda, O. Kitao, H. Nakai, M. Klene, X. Li, J.E. Knox, H.P. Hratchian, J.B. Cross, C. Adamo, J. Jaramillo, R. Gomperts, R.E. Stratmann, O. Yazyev, A.J. Austin, R. Cammi, C. Pomelli, J.W. Ochterski, P.Y. Ayala, K. Morokuma, G.A. Voth, P. Salvador, J.J. Dannenberg, V.G. Zakrzewski, S. Dapprich, A.D. Daniels, M.C. Strain, O. Farkas, D.K. Malick, A.D. Rabuck, K. Raghavachari, J.B. Foresman, J.V. Ortiz, Q. Cui, A.G. Baboul, S. Clifford, J. Cioslowski, B.B. Stefanov, G. Liu, A. Liashenko, P. Piskorz, I. Komaromi, R.L. Martin, D.J. Fox, T. Keith, M.A. Al-Laham, C.Y. Peng, A. Nanayakkara, M. Challacombe, P.M.W. Gill, B. Johnson, W. Chen, M.W. Wong, C. Gonzalez, J.A. Pople, Gaussian 03, Revision B.04, Gaussian, Inc., Wallingford CT, 2004.
- [19] (a) A.D. Becke, *Phys. Rev. A* 38 (1988) 3098–3100;
(b) C. Lee, W. Yang, R.G. Parr, *Phys. Rev. B* 37 (1988) 785–789.
- [20] (a) R.M. Edkins, A. Wriglesworth, K. Fucke, S.L. Bettington, A. Beeby, *Dalton Trans.* 40 (2011) 9672–9678;
(b) V. Chandrasekhar, B. Mahanti, P. Bandipalli, K. Bhanuprakash, *Inorg. Chem.* 51 (2012) 10536–10547;
(c) E.A. Plummer, J.W. Hofstraat, L.D. Cola, *Dalton Trans.* (2003) 2080–2084.
- [21] X. Shen, F.L. Wang, F. Sun, R. Zhao, X. Wang, S. Jing, Y. Xu, D.R. Zhu, *Inorg. Chem. Commun.* 14 (2011) 1511–1515.
- [22] D.P. Rillema, D.G. Taghdiri, D.S. Jones, C.D. Keller, L.A. Worl, T.J. Meyer, H.A. Levy, *Inorg. Chem.* 26 (1987) 578–585.
- [23] K.A. King, P.J. Spellane, R.J. Watts, *J. Am. Chem. Soc.* 107 (1985) 1431–1432.